Evaluating methods for representing model error using ensemble data assimilation

Jeffrey S. Whitaker and Thomas M. Hamill

NOAA Earth System Research Laboratory/Physical Sciences Division
Boulder CO, USA
Jeffrey.S.Whitaker@noaa.gov

ABSTRACT

Inflation of ensemble perturbations is often employed in ensemble Kalman filters to account for unrepresented error sources. We present a new multiplicative inflation algorithm that inflates the posterior ensemble in proportion to the amount that observations reduce the ensemble spread, resulting in more inflation in regions of dense and/or accurate observations. This is justified since sampling and model error are expected to be a larger fraction of the total background error in these regions. The algorithm is similar to the 'relaxation-to-prior algorithm proposed by Zhang et al, but it relaxes the posterior ensemble *spread* back to the prior, instead of the posterior ensemble perturbations.

The new inflation algorithm is compared to the method of Zhang et al and simple constant covariance inflation using a two-level spherical primitive equation model in an environment that includes model error. We find the new method performs best and is less sensitive to variations of the inflation parameter around the optimal value. Combining the new multiplicative inflation algorithm with additive inflation (adding random perturbations drawn from a specified distribution to the ensemble) is found to superior to either of the methods used separately.

It is argued that multiplicative inflation is best suited to account for unrepresented observation network dependent assimilation errors, while model errors (which do not depend on the observing network) are best treated by additive inflation, or stochastically within the forecast model itself. A combination of additive and multiplicative inflation can provide a baseline for evaluating more sophisticated stochastic treatments of unrepresented background errors. This is demonstrated by comparing the performance of a stochastic kinetic energy backscatter scheme with additive inflation as a parameterization of model error in this simplified environment.

1 Introduction

The ensemble Kalman filter (EnKF) is an approximation to the Kalman filter, in which the background-error covariance is estimated from an ensemble of short-term model forecasts. The use of EnKF data assimilation systems to initialize ensemble weather predictions is growing e.g. (Whitaker et al., 2008; Hamill et al., 2011; Houtekamer et al., 2005, 2009; Buehner et al., 2010), because of the simplicity of the algorithm and it's ability to provide *flow-dependent* estimates of background and analysis error. In the EnKF, it is assumed that the background (prior) ensemble samples all sources of error in the forecast environment, including sampling error due to limitations in ensemble size, and errors in the model itself. Inevitably, some sources of error will be under-sampled, resulting in a sub-optimal EnKF with too little spread. An EnKF with too little spread will not give enough weight to observations, which in a chaotic system will cause the subsequent ensemble forecasts to drift farther from the truth. At the next assimilation time, the ensemble spread will be even more deficient, causing the update to give even less weight to observations. This problem can progressively worsen, potentially resulting in a condition called 'filter divergence', in which the ensemble variance becomes vanishingly small and observation information is completely ignored. Because of this, all EnKF systems used in weather prediction employ methods to account of unrepresented or underestimated error sources in the prior

ensemble. These include multiplicative inflation (Anderson and Anderson, 1999), which inflates either the prior or posterior ensemble by artificially increasing the amplitude of deviations from the ensemble mean, or additive inflation, which involves adding random perturbations with zero mean from a specified distribution to each ensemble member. Whitaker et al. (2008) compared simple uniform multiplicative inflation with additive inflation in a simple model, and found that additive inflation performed better, since the simple uniform multiplicative inflation generated too much spread in regions less constrained by observations. Houtekamer et al. (2009) compared additive inflation with various methods for treating model error within the forecast model itself (such as multi-model ensembles, stochastic-backscatter (Shutts, 2005; Berner et al., 2009) and stochastically perturbed physics tendencies (Buizza and Palmer, 1999)). They found that additive inflation, sampling from a simple isotropic covariance model, had the largest positive impact. However, Hamill and Whitaker (2010) found that parameterizing unrepresented error sources with additive inflation will decrease the flow-dependence of background-error covariance estimates and reduce the growth rate of ensemble perturbations, with potentially negative consequences on analysis quality.

Here we revisit the use of multiplicative covariance inflation, with some simple theory as a guide. Sacher and Bartello (2008) showed that sampling error in the estimate of the Kalman gain should be proportional to the amplitude of the Kalman gain itself, so that more inflation is needed when observations are making large corrections to the background. More generally, since the assimilation of observations will result in a reduction of ensemble spread, those sources of background error (such as model error) that do not depend on the characteristics of the assimilation system itself, such as the observing network, should be a relatively larger fraction of background error in regions of dense and/or accurate observations. This was illustrated in a simple 1-d Kalman filter by Daley and Ménard (1993). In that paper, an advective-diffusion equation with a uniform model-error covariance was used to derive a scalar equation for the background-error variance as a function of spectral wavenumber (their equation 2.11) of the form

$$f_{n+1}^2 = m(1-k_n)f_n^2 + q^2 = \frac{mr^2 f_n^2}{r^2 + f_n^2} + q^2, \tag{1}$$

where k_n is the Kalman gain at time level n, f_n^2 is the prior variance at time level n, r^2 is the observation error variance, m is the linear model operator and q^2 is the model-error variance. For a given value of the prior variance at time level n, the model error variance will become a larger fraction of the prior variance at the next time level as the observation error variance is decreased (and the Kalman gain is increased). Therefore, if model error is to parameterized as a multiplicative inflation (i.e a constant times f_n^2) that constant should be larger when observations have a larger impact, that is when observations are dense and/or accurate.

Zhang et al. (2004) proposed an alternative to simple covariance inflation that relaxes posterior (analysis) perturbations back toward the prior (first guess) perturbations independently at each analysis point via

$$\mathbf{x}_i^{'a} \leftarrow (1-\alpha)\mathbf{x}_i^{'a} + \alpha\mathbf{x}_i^{'b}, \tag{2}$$

where $\mathbf{x}_i^{'a}$ is the deviation from the posterior ensemble mean for the i^{th} ensemble member, and $\mathbf{x}_i^{'b}$ is the deviation from the prior ensemble mean for the i^{th} ensemble member. We refer to this method as "relaxation-to-prior perturbations" (RTPP). Unlike simple covariance inflation, this technique has the desired property of increasing the posterior ensemble variance in proportion to the amount that the assimilation of observations has reduced the prior variance. In the limit that α approaches 1.0, the posterior ensemble is completely replaced the prior ensemble. For values of α between 0 and 1, part of the posterior ensemble is replaced by the prior ensemble. This approach amounts to a combination of multiplicative iWhitakernflation (in which the inflation factor is less than 1) and additive inflation where the perturbations are taken from the prior ensemble. Here we propose a new approach, which we call "relaxation-to-prior spread" (RTPS), that is a purely multiplicative inflation. Instead of relaxing the posterior *perturbations* back to their prior values at each grid point as in RTPP, we relax the ensemble

standard deviation back to the prior via

$$\sigma^a \leftarrow (1-\alpha)\sigma^a + \alpha\sigma^b, \tag{3}$$

where $\sigma^b \equiv \sqrt{\frac{1}{n-1}\sum_{i=1}^{n} \mathbf{x}_i^{'b2}}$ and $\sigma^a \equiv \sqrt{\frac{1}{n-1}\sum_{i=1}^{n} \mathbf{x}_i^{'a2}}$ are the prior and posterior ensemble standard deviation (spread) at each analysis grid point, and n is the ensemble size. This formula can be rewritten

$$\mathbf{x}_i^{'a} \leftarrow \mathbf{x}_i^{'a}\sqrt{\alpha\frac{\sigma^b - \sigma^a}{\sigma^a} + 1}. \tag{4}$$

For a given value of α, the multiplicative inflation is proportional to the amount the ensemble spread is reduced by the assimilation of observations, normalized by the posterior ensemble spread. Anderson (2009) proposed a Bayesian algorithm for estimating a spatially and temporally varying field of covariance inflation as part of the state update. When run as part of an EnKF assimilation system using a global general circulation model with all "conventional" (i.e. non satellite radiance) observations, the Bayesian algorithm produces a spatial field of inflation that looks very similar to that implied by RTPS inflation (equation 4), with large values of inflation in regions of dense and/or accurate observations, like North America and Europe (Figure 13 in Anderson et al. (2009)).

In the following, the proposed new multiplicative inflation algorithm (RTPS, equation 4) is compared to the RTPP method of Zhang et al. (2004), the adaptive inflation algorithm of Anderson (2009), and simple constant covariance inflation using the serial ensemble square-root filter of Whitaker and Hamill (2002) in an idealized 2-level primitive equation model on a sphere, including model error. The RTPS inflation algorithm is found to produce more accurate analyses than either RTPP or constant inflation, with analysis errors similar to the adaptive algorithm. Additive inflation outperforms all of the multiplicative methods. However, a combination of the RTPS multiplicative inflation and additive inflation performs better than either alone. Further experiments with reduced sampling error (using a much larger ensemble) and reduced model error (using a perfect model in the assimilation system) are conducted to investigate the relative utility of additive and multiplication inflation. It is found that unrepresented observation network dependent assimilation errors (which in this simple case comes from only sampling error) are best handled by multiplicative inflation, while model errors (which do not depend on the observing network) are best treated by additive inflation. As an alternative to additive inflation, it seems preferable to represent model errors within the forecast model itself using techniques like those described in Berner et al. (2009) and Buizza and Palmer (1999). Some results with the stochastic backscatter scheme (Berner et al., 2009) are presented to test this conjecture. The results show that a combination of additive and multiplicative inflation is surprisingly hard to improve upon, and can server as baseline for evaluation of more sophisticated methods for represented under-represented sources of error in ensemble data assimilation systems.

2 Idealized experiments

2.1 Forecast model

The forecast model used in these experiments is virtually identical to the two-level primitive equation spectral model of Lee and Held (1993). This model was also used in the data assimilation experiments of Whitaker and Hamill (2002) and Hamill and Whitaker (2010). Here, unless otherwise noted, data assimilation experiments are run with a spectral resolution of T31 (triangular truncation at total wavenumber 31), with the two levels set to 250 and 750 hPa. Observations are sampled from a nature run using the same model, but at T42 resolution. The prognostic variables of the forecast model are baroclinic

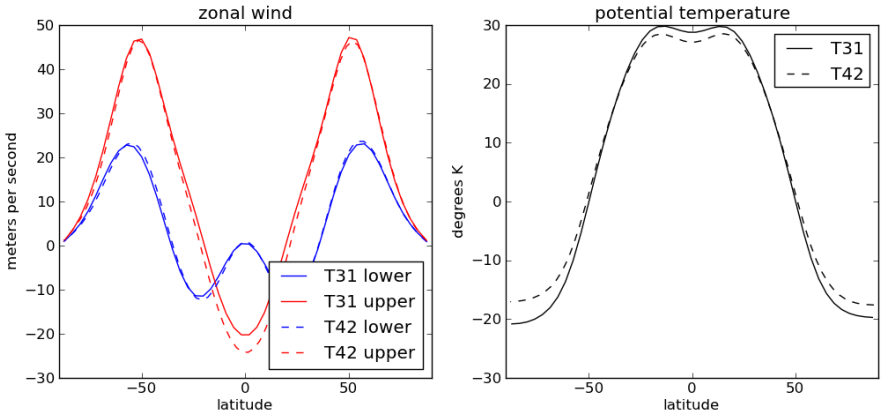

Figure 1: Zonal and time mean zonal wind (left) and potential temperature (right) for the two-level model run at T31 and T42 resolution.

and barotropic vorticity, baroclinic divergence, and barotropic potential temperature. Barotropic divergence is identically zero, and baroclinic potential temperature (static stability) is kept constant at 10K. Lower-level winds are mechanically damped with an e-folding timescale of 4 days, and barotropic potential temperature is relaxed back to a radiative equilibrium state with a pole-to-equator temperature difference of 80K with a timescale of 20 days. The radiative equilibrium profile of Lee and Held (1993) (equation 3) was used. ∇^8 diffusion was applied to all the prognostic variables, the smallest resolvable scale is damped with an e-folding timescale of 3 hours (6 hours for the nature run). Time integration is performed with a 4th–order Runge-Kutta scheme with 18 time steps per day at T31 resolution, and 30 at T42 resolution. The error doubling time of the T31 model is approximately 2.4 days. The climate of the model (computed as a zonal and time mean over 1000 days of integration) is shown in Figure 1 for the T31 forecast model and the T42 nature run. The time-mean systematic error of the T31 model is quite small outside the tropics and polar regions.

2.2 Data assimilation methodology

The serial ensemble square-root filter algorithm of Whitaker and Hamill (2002) is used in conjunction with a 20 member ensemble, unless otherwise noted. Details are provided in Hamill and Whitaker (2010). Covariance localization (Hamill et al., 2001) is used to ameliorate the effects of sampling error, using the compact Gaussian-like polynomial function of Gaspari and Cohn (1999). Observations of geopotential height at 250 and 750 hPa are assimilated at Northern Hemisphere radiosonde locations (Figure 2) every 12 hours with an observation error standard deviation of 10 meters. The observing network is made hemispherically symmetric by reflecting the Northern Hemisphere radiosonde locations into the Southern Hemisphere, resulting in a network with 1022 observing locations.

2.3 Comparison of multiplicative inflation methods.

Experiments were conducted with three different methods of multiplicative inflation (simple covariance inflation, RTPP and RTPS) to account for background errors not account for by the first-guess ensemble, which in this case includes both sampling error and model error, since the assimilating model is run at lower resolution than the model used to generate the observations. In all of these experiments, the covariance localization was set so that increments taper to zero 3500 km away from observation locations.

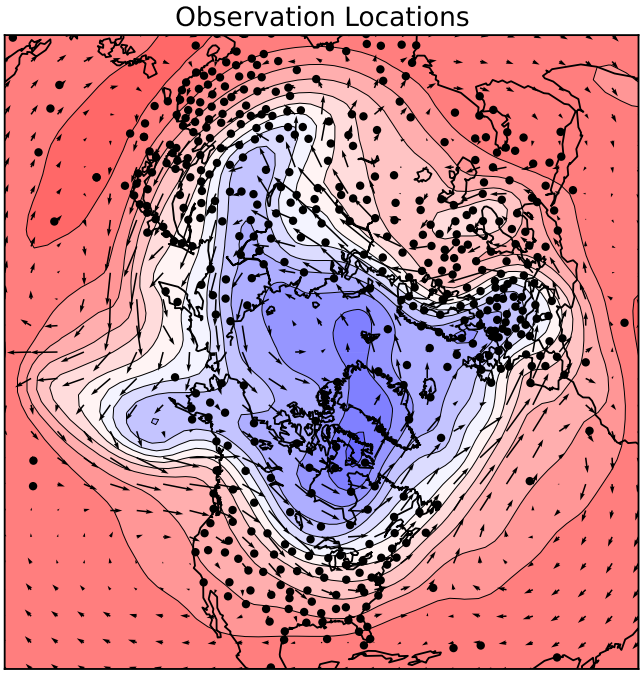

Figure 2: Observation locations (black dots) superimposed upon a snapshot of barotropic potential temperature (shaded contours every 5K) and upper-level winds (vectors) from the T42 nature run used in the two-level model data assimilation experiments. Continental outlines are shown for reference, even though the model has no orography or land-sea contrast. Data is plotted on a azimuthal equidistant map projection centered on the North Pole.

This is close to the optimal value for all of the three inflation methods. Ensemble mean error and spread are calculated using the total energy norm

$$E(\overrightarrow{V_1},\overrightarrow{V_2},\theta_{3/2}) = \frac{1}{2}(u_1^2+v_1^2)+\frac{1}{2}(u_2^2+v_2^2)+\frac{\triangle\bar{\pi}}{\triangle\bar{\theta}}\theta_{3/2}^2, \tag{5}$$

where $\triangle\bar{\theta}$ is the constant static stability (10K), $\triangle\bar{\pi}$ is the difference in Exner function between the lower level (750 hPa) and the upper level (250 hPa), $\overrightarrow{V_1} = (u_1, v_1)$ is the lower level horizontal velocity vector, and $\overrightarrow{V_2} = (u_2, v_2)$ is the upper level velocity, and $\theta_{3/2}$ is the barotropic, or mid-level potential temperature. Ensemble mean error is computed by replacing the velocity and potential temperature in equation 5 by the difference between the ensemble mean and the truth (as defined by the T42 nature run). The ensemble spread is computed by replacing the velocity and potential temperature in equation 5 by the difference between each ensemble member and the ensemble mean, then summing over each ensemble member and dividing by the number of ensemble members minus one. Global and time means of the resulting quantities are computed, and a square root is then applied so that the result has units of meters per second.

Figure 3 shows ensemble mean background error and spread statistics collected over 1000 assimilation times for the three experiments, after a spinup period of 50 days. The RTPS inflation method produces more accurate analyses and short-term forecasts than either RTPP and constant covariance inflation, and is less sensitive to variations of the inflation parameter about it's optimal value (the value at which the ensemble mean error is minimized). RTPP outperforms constant covariance inflation, but produces

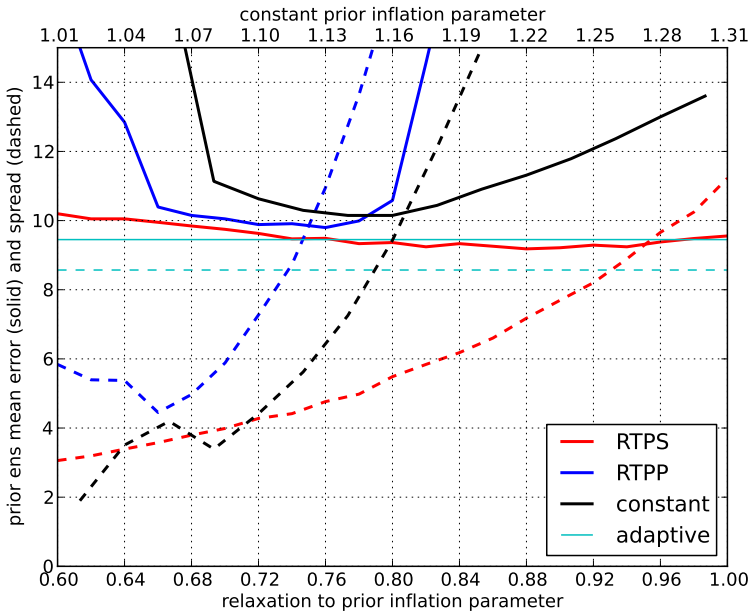

Figure 3: Ensemble mean background error and spread (in terms of the square-root of total energy norm in ms^{-1}) for two-level model assimilation experiments using relaxation-to-prior perturbation (RTPP) inflation (blue), relaxation-to-prior standard deviation (RTPS) inflation (red), and simple constant covariance inflation (black). The solid lines denote ensemble mean error and the dashed lines denote ensemble spread. The values of the inflation parameter for RTPP and RTPS are given on the lower x-axis, while the values of the constant covariance inflation parameter are given on the upper x-axis. All experiments used covariance localization that tapers covariances to zero 3000 km away from observations locations, and were run for 1000 assimilation steps, after an initial spinup period of 50 days. The definition of the total energy norm is given in the text.

very large errors when the inflation parameter exceeds the optimal value. The ensemble spread for all three experiments is less than the ensemble mean error when ensemble mean error is at its minimum (the dashed lines are below the solid lines at the minimum in the solid line), indicating the ensembles are slightly under-dispersive when they are optimized for ensemble mean error. Both the ensemble spread and ensemble mean error for the RTPS inflation appears to be less sensitive to variations in the inflation parameter. For reference, we also show in Figure 3 the ensemble mean error and spread for an experiment using the adaptive inflation algorithm of Anderson (2009) (the horizontal cyan curves). The adaptive inflation algorithm requires very little tuning (there is some sensitivity to the value of the prior inflation variance chosen), and produces analysis of similar quality to the best-tuned RTPS results.

RTPP inflation has at least one desirable property - it produces ensemble perturbations that grow faster than the other inflation methods. This is illustrated in Figure 4, which shows that ratio of background spread to analysis spread for the experiments depicted in Figure 3. At the minimum in ensemble mean error, the RTPP ensemble spread grows about 19% during over the assimilation interval (12 hours), compared to 7.6% for RTPS inflation and 6.5% for simple covariance inflation. The reason for this can be understood by noting that RTPP inflation involves adding scaled prior perturbations to the posterior ensemble. When the inflation parameter α is 1, the posterior ensemble is completely replaced by the prior ensemble. In that case, the structure and amplitude of the ensemble perturbations is not modified during the assimilation and the perturbations are simply re-centered around the updated ensemble mean. The assimilation cycle then becomes very similar to the process used to compute the leading Lyapunov vector (Legras and Vautard, 1995), which reflect the dominant instabilities of a dynamical system. This

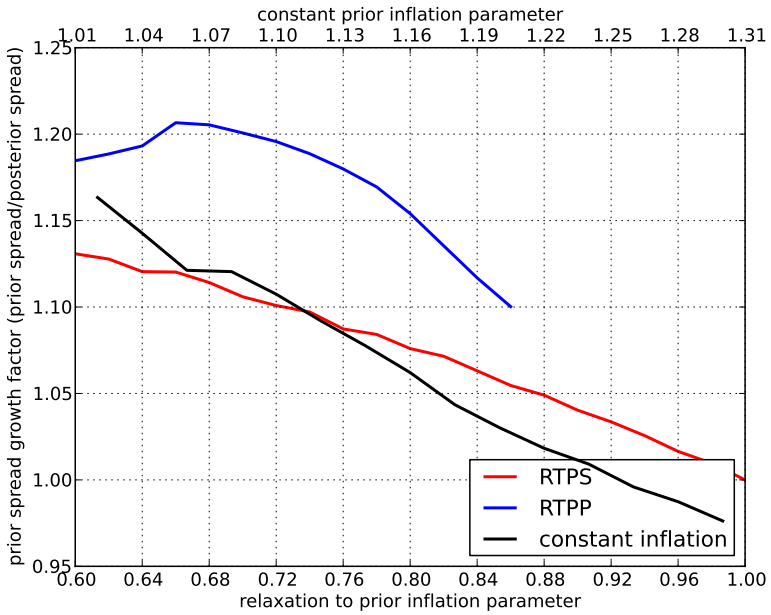

Figure 4: As in Figure 2, but instead of ensemble mean background error and spread, the ratio of background spread to analysis spread (the spread growth factor) is plotted as a function of the inflation parameter.

also explains why the performance of RTPP inflation degrades rapidly when the inflation parameter is increased above the optimal value - the ensemble perturbations become increasingly co-linear as they collaps to the leading Lyapunov vector, reducing the effective number of degrees of freedom spanned by the ensemble. However, Figure 4 shows that the spread growth does not increase for RTPP inflation monotonically as the inflation parameter is increased - this is because the amplitude of the ensemble perturbations becomes large enough that nonlinear effects begin to cause saturation.

To further explore the impact of the multiplicative inflation method on the growth properties of the analysis ensemble, we have calculated the analysis-error covariance singular vector (AECSV) spectrum following the methodology of Hamill et al. (2003). The AECSVs are the structures that explain the greatest forecast variance and whose initial size is consistent with the flow-dependent analysis-error covariance statistics of the data assimilation system. Figure 5 confirms that the RTPP ensemble AECSV spectrum is steeper, with more of the variance concentrated in fewer, faster growing modes. The leading AECSV for the RTPS ensemble grows just as rapidly as the leading AECSV in the RTPP ensemble, but the trailing ones grow much slower. This results in less spread growth over the assimilation interval, but an ensemble that can effectively span a larger portion of the space of possible analysis errors.

2.4 Combined additive and multiplicative inflation.

In Hamill and Whitaker (2005), it was found that additive inflation performed better than constant covariance inflation in a idealized 2-layer primitive equation model, including truncation model error. Similarly, Whitaker et al. (2008) found that additive inflation outperformed constant covariance inflation and RTPP inflation in a full global numerical weather prediction system. Given that RTPS inflation performs better than RTPP and constant covariance inflation, how does it perform compared to additive inflation? Here we use random samples from a climatological distribution of actual 12-h forecast model error for our additive inflation. The distribution is computed using the same method as Hamill

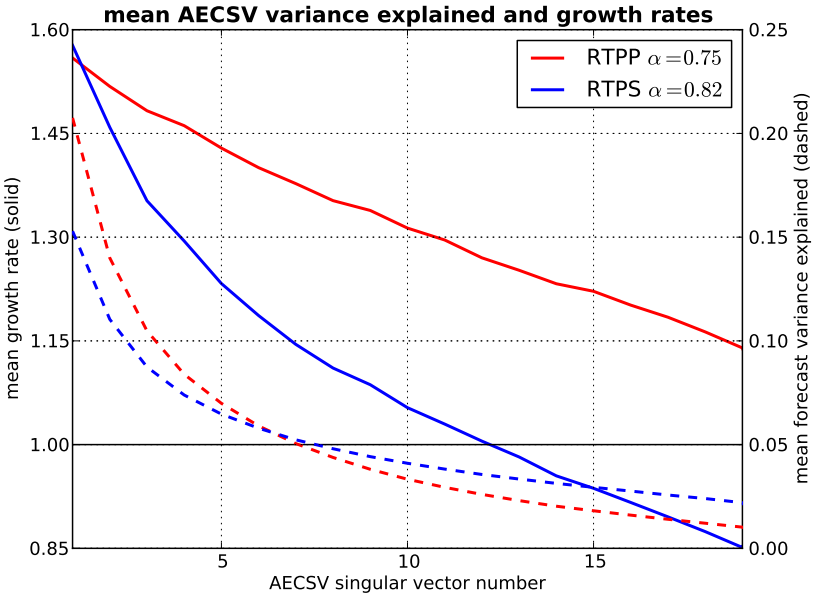

Figure 5: The mean analysis error covariance singular vector (AECSV) spectrum for RTPP analysis ensembles with $\alpha = 0.75$ (red) and RTPS analysis ensembles with $\alpha = 0.82$ (blue). The solid lines represent the mean growth rates (left y-axis), and the dashed lines represent the mean background forecast variance explained (right y-axis) as a function as AECSV singular value number.

and Whitaker (2005), that is by truncating the T42 nature run to T31, running 12-h forecasts at T31 and computing the difference between these forecasts and the corresponding T31 truncated nature run fields. The only source of error in these forecasts is due to the lower resolution of the forecast model. At each analysis time, 20 samples are chosen randomly from this distribution, the mean is removed, and the resulting fields are scaled and added to each ensemble member. Figure 6 shows the ensemble background error for experiments using a combination of this additive inflation and RTPS multiplicative inflation. The additive inflation parameter is simply the scaling factor applied to the randomly chosen truncation model error fields. The values of ensemble mean error when the additive inflation parameter is zero are identical to those shown in Figure 3 (the solid red line). From this plot, it is easy to see that additive inflation without multiplicative inflation produces lower errors than multiplicative inflation alone, in agreement with he results of Hamill and Whitaker (2005) and Whitaker et al. (2008). However, a combination of additive and multiplicative inflation produces lower errors than either method used alone. The minimum error (8.6 ms^{-1}) occurs with a multiplicative inflation parameter of 0.5 and an additive inflation parameter of 1.4. Conditioning the additive perturbations to the dynamics by adding them to the previous ensemble mean analysis (instead of the current analysis) and evolving them forward in time one assimilation interval (as suggested by Hamill and Whitaker (2010)) reduces the minimum error slightly, by approximately 2-3% (not shown). Using random samples of 12-h differences drawn from a T31 model run works nearly as well as using actual truncation model error fields for the additive inflation, yielding a minimum error of (8.8 ms^{-1}) when the additive inflation parameter is 0.24 and the multiplicative inflation parameter is 0.5 (Figure 7).

The fact that a combination of additive and multiplicative inflation works better than either alone suggests that they are representing different unrepresented background-error sources. RTPS multiplicative inflation is by design dependent on the observation network, while the additive inflation we have used is independent of the assimilation system. Therefore, we hypothesize that RTPS multiplicative inflation is useful in capturing unrepresented sources of error that depend on the assimilation system, such

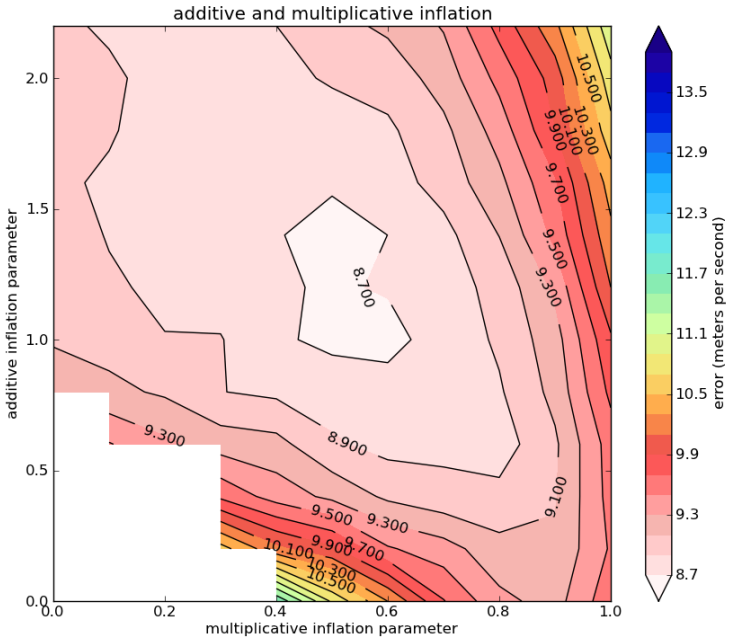

Figure 6: Contours of ensemble mean background error using a combination of multiplicative and additive inflation. The additive inflation is created by drawing samples from a distribution of actual 12-h forecast model errors. The multiplicative inflation parameter varies along the x-axis, while the additive inflation parameter varies along the y-axis. The solid red line in Figure 3 is a cross-section along y=0 in this plot. See text for details. Filter divergence occurs where no contours are plotted.

as sampling error, while additive inflation is useful in capturing sources of background error that are assimilation-system independent, such as errors in the forecast model. To test this idea we ran two experiments: one in which the model error was eliminated by using the T42 model in the assimilation, and another in which the sampling error was reduced by increasing the ensemble size from 20 to 200. In the former experiment, we expect that the relative impact of additive inflation would be reduced relative to multiplicative inflation, since the only source of unrepresented source of error (sampling error) comes from the data assimilation system itself. In the latter experiment, sampling error is greatly reduced, so that the dominant unrepresented source of error should be model error and the impact of multiplicative inflation should be reduced relative to additive inflation. These expectations are confirmed in Figures 8 and 9. Figure 8 shows that in the absence of model error, multiplicative inflation alone outperforms any combination of multiplicative and additive inflation. Figure 9 shows that when model error is the dominant source of unrepresented background errors, additive inflation alone outperforms any combination of multiplicative and additive inflation.

2.5 Replacing additive inflation with stochastic backscatter.

The additive inflation algorithm used here is somewhat ad-hoc, and it would be preferable to incorporate a physically-based parameterization of model error directly into the forecast model. Such a parameterization would account for the presence of model error directly in the background ensemble forecast. The only source of error in our two-level model experiments is associated with model truncation. More specifically, model error in our experiments is a result of the effects of unresolved and unrealistically damped scales on the resolved scales through an inverse energy cascade. This is exactly the sort of model error that stochastic kinetic energy backscatter (SKEB) schemes (Shutts, 2005; Berner et al., 2009) were

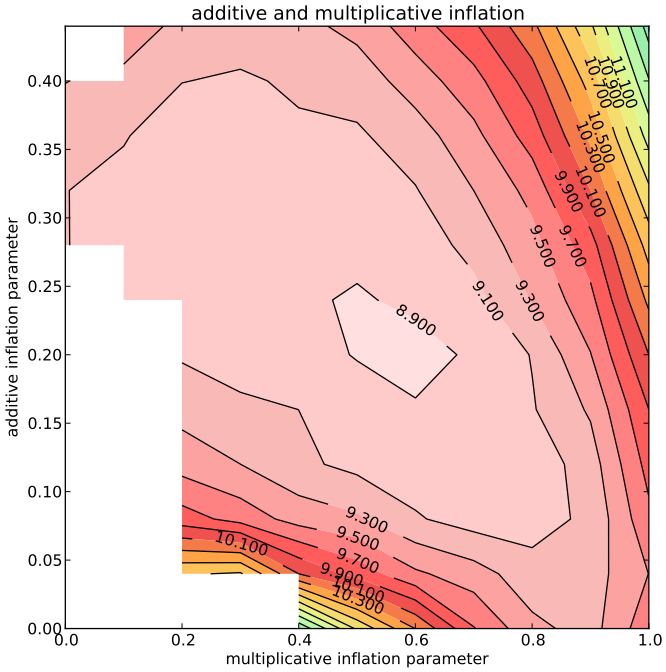

Figure 7: As in Figure 6, but additive inflation is created by drawing samples from the climatological distribution of T31 model 12-h.

designed to represent. The algorithm described by Berner et al. (2009) involves generating a random streamfunction pattern from an AR-1 process with a specified timescale and covariance structure. These random patterns are then modulated by the model's kinetic energy dissipation rate (resulting from the ∇^8 hyperdiffusion). The resulting tendencies are added as forcing term in the vorticity equation. Figure 10 shows the the total kinetic energy spectra for the T42 model, the T31 model without SKEB, and the T31 model with SKEB. The kinetic energy in the T31 model without SKEB is deficient relative to the T42 model at all scales, but especially so near the truncation wavenumber where the hyperdiffusion is active. Adding SKEB to the T31 model brings the energy up much closer to the level of the T42 model. The random streamfunction pattern used to generate the SKEB forcing was assumed to be spatially white in the streamfunction norm, with a decay timescale of 6 hours. The amplitude of the random streamfunction pattern was set to 15, a value chosen to give the best fit to the T42 model kinetic energy spectrum shown in Figure 10.

Figure 11 show the results for a set of assimilation experiments using a combination of SKEB to represent model error, and multiplicative inflation to represent other sources of unrepresented background errors (in this case, primarily sampling errors). Not surprisingly, a combination of SKEB and multiplicative inflation turns out to be better than either alone. However, comparing Figure 11 to Figure 7, SKEB does not seem to perform significantly better than simple, ad-hoc additive inflation. Also, in contrast to the additive inflation case, SKEB alone does not perform better than additive inflation alone. Of course, there are several tunable parameters in the SKEB scheme (including the total variance injected, the timescale of the random streamfunction pattern, and the covariance structure of the random streamfunction pattern) and it likely that better results could be obtained by more carefully tuning these parameters. However, our results do suggest that it is surprisingly hard to beat a combination of simple additive and multiplicative inflation as a parameterization of unrepresented sources of error in an ensemble data assimilation system.

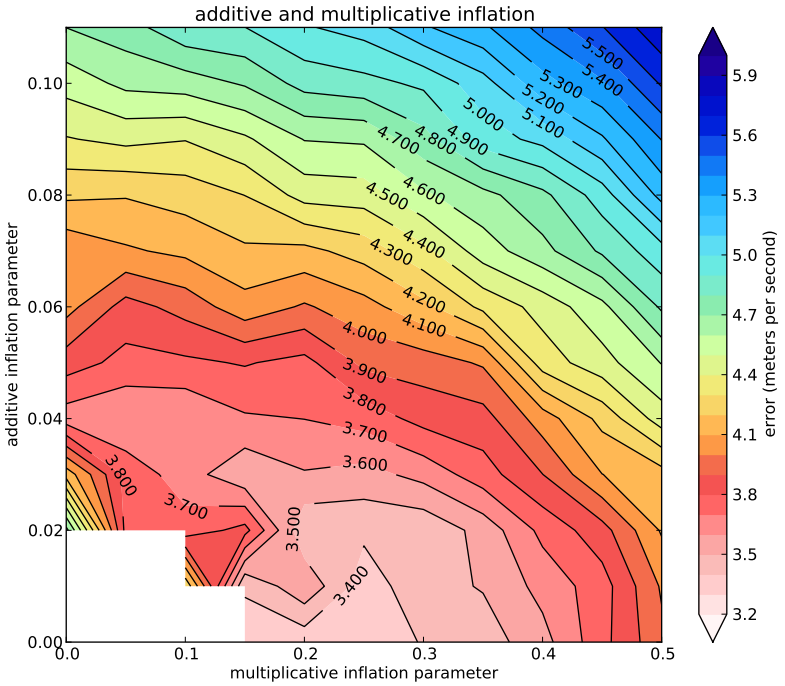

Figure 8: As in Figure 7, but for a "perfect model" experiment in which the T42 model is used in the data assimilation.

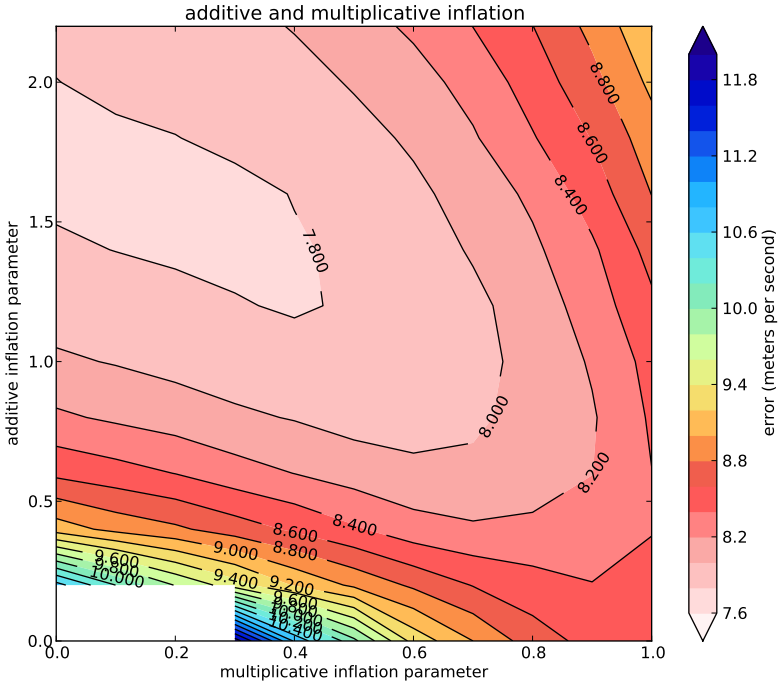

Figure 9: As in Figure 7, but the ensemble size in the data assimilation is increased from 20 to 200.

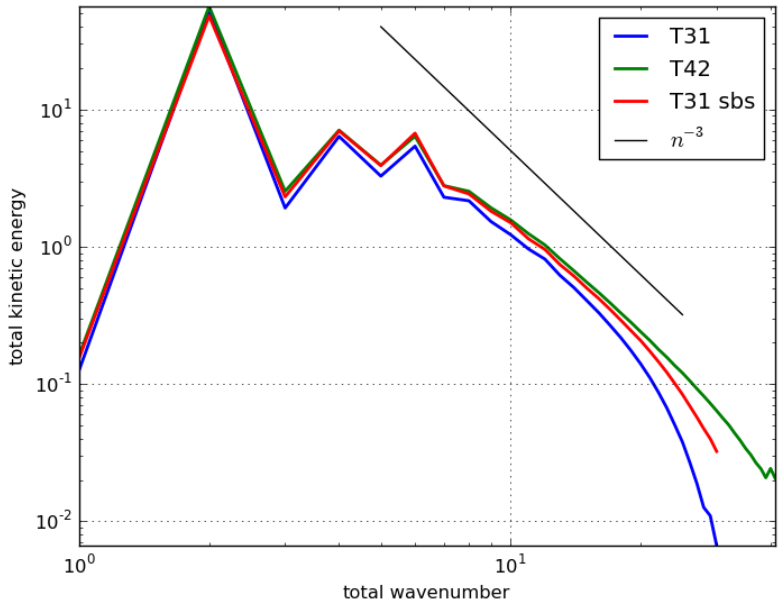

Figure 10: Total kinetic energy spectra as a function of total wavenumber for the T31 model (blue) the T42 model (green) and the T31 model with stochastic kinetic energy backscatter (red). See text for details. For reference, a line representing a -3 power-law spectrum characteristic of 2D turbulence is shown in black.

3 Conclusions

In the EnKF, it is assumed that the background (prior) ensemble samples all sources of error in the forecast environment, including those associated with the data assimilation itself (such as sampling error due to finite ensemble size, mis-specification of observation errors and errors in forward operators) as well as errors in the forecast model itself. We have proposed a new multiplicative inflation algorithm to treat these unrepresented sources of error that is simple to implement in complicated models. Using idealized experiments with a two-level spherical primitive equation model, where the only source of model error is associated with model truncation, and the only source of data assimilation error is associated with finite ensemble size, we show that this new inflation scheme performs as well or better than other commonly used schemes. It has the desirable property of inflating more strongly where the assimilation of observations has a larger effect on the ensemble variance. It is in these regions where both model and sampling error are expected to be a larger fraction of the total background error.

Combining this new multiplicative inflation algorithm with additive inflation, it is found that a combination of the two performs better than either alone, even when the additive perturbations are drawn from an ad-hoc distribution that does not directly use knowledge of the known properties of the model error in this simplified environment. This leads us to hypothesize that multiplicative inflation is best suited to account for unrepresented observation network dependent assimilation errors, while model errors (which do not depend on the observing network) are best treated by additive inflation, or stochastically within the forecast model itself. Since the additive inflation algorithm is somewhat ad-hoc, it is expected that a more physically-based parameterization of model error, such as stochastic kinetic energy backscatter, will perform better. Tests replacing additive inflation with SKEB in the data assimilation show that it is surprisingly hard to improve upon additive inflation. This suggest that a combination of simple ad-hoc additive inflation with the new multiplication inflation algorithm proposed here can provide a rigorous baseline for testing new more sophisticated representations of unrepresented sources of error

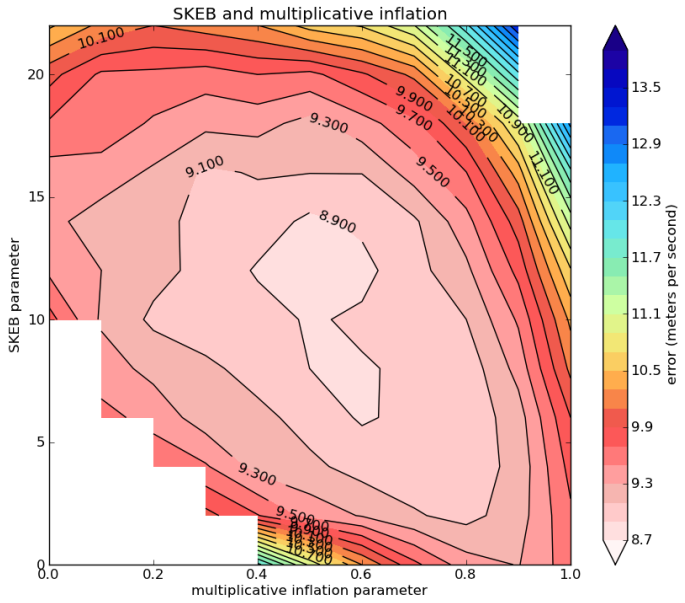

Figure 11: Contours of ensemble mean background error using a combination of multiplicative inflation and stochastic kinetic energy backscatter (SKEB). The multiplicative inflation parameter varies along the x-axis, while the amplitude of the SKEB forcing varies along the y-axis. The solid red line in Figure 3 is a cross-section along y=0 in this plot. See text for details. Filter divergence occurs where no contours are plotted.

in ensemble data assimilation systems.

References

Anderson, J. L. (2009). Spatially and temporally varying adaptive covariance inflation for ensemble filters. *Tellus A 61*, 72–83.

Anderson, J. L. and S. L. Anderson (1999). A Monte Carlo implementation of the nonlinear filtering problem to produce ensemble assimilations and forecasts. *Mon. Wea. Rev. 127*, 2741–2758.

Anderson, J. L., T. Hoar, K. Raeder, H. Liu, N. Collins, R. Torn, and A. Avellano (2009, January). The data assimilation research testbed: A community facility. *Bull. Amer. Meteor. Soc. 90*, 1283–1296.

Berner, J., G. J. Shutts, M. Leutbecher, and T. N. Palmer (2009). A spectral stochastic kinetic energy backscatter scheme and its impact on flow-dependent predictability in the ecmwf ensemble prediction system. *J. Atmos. Sci. 66*, 603–626.

Buehner, M., P. L. Houtekamer, C. Charette, H. L. Mitchell, and B. He (2010). Intercomparison of variational data assimilation and the ensemble kalman filter for global deterministic nwp. part i: Description and single-observation experiments. *Mon. Wea. Rev. 138*, 1902–1921.

Buizza, R. and T. N. Palmer (1999). Stochastic representation of model uncertainties in the ECMWF ensemble prediction system. *Quart. J. Roy. Meteor. Soc. 125*, 2887–2908.

Daley, R. and R. Ménard (1993). Spectral characteristics of kalman filter systems for atmospheric data assimilation. *Mon. Wea. Rev. 121*, 1554–1565.

Gaspari, G. and S. E. Cohn (1999). Construction of correlation functions in two and three dimensio ns. *Quart. J. Roy. Meteor. Soc. 125*, 723–757.

Hamill, T., C. Snyder, and J. S. Whitaker (2003). Ensemble forecasts and the properties of flow-dependent analysis-error covariance singular vectors. *Mon. Wea. Rev. 131*, 1741–1758.

Hamill, T. M. and J. S. Whitaker (2005). Accounting for the error due to unresolved scales in ensemble data assimilation: A comparison of different approaches. *Mon. Wea. Rev. 133*, 3132–3147.

Hamill, T. M. and J. S. Whitaker (2010). What constrains spread growth in forecasts initialized from ensemble Kalman filters? *Monthly Weather Review 138*, to appear.

Hamill, T. M., J. S. Whitaker, M. Fiorino, and S. G. Benjamin (2011). Global ensemble predictions of 2009's tropical cyclones initialized with a ensemble Kalman filter. *Mon. Wea. Rev. 139*, to appear.

Hamill, T. M., J. S. Whitaker, and C. Snyder (2001). Distance-dependent filtering of background error covariance estimates in an ensemble Kalman filter. *Mon. Wea. Rev. 129*, 2776–2790.

Houtekamer, P. L., H. L. Mitchell, and X. Deng (2009). Model error representation in an operational ensemble kalman filter. *Mon. Wea. Rev. 137*, 2126–2143.

Houtekamer, P. L., H. L. Mitchell, G. Pellerin, M. Buehner, M. Charron, L. Spacek, and B. Hansen (2005). Atmospheric data assimilation with an Ensemble Kalman Filter: Results with real observations. *Mon. Wea. Rev. 133*, 604–620.

Lee, S. and I. M. Held (1993). Baroclinic wave packets in models and observations. *J. Atmos. Sci. 50*, 1413–1428.

Legras, B. and R. Vautard (1995). A guide to Lyapunov vectors. In *Proc. ECMWF Seminar on Predictability*, Volume 1, Reading, United Kingdom, pp. 143–156. ECMWF.

Sacher, W. and P. Bartello (2008). Sampling errors in ensemble kalman filtering. part i: Theory. *Mon. Wea. Rev. 136*, 3035–3049.

Shutts, G. (2005). A kinetic energy backscatter algorithm for use in ensemble prediction systems. *Quart. J. Roy. Meteor. Soc. 131*, 3079–3102.

Whitaker, J. S. and T. M. Hamill (2002). Ensemble data assimilation without perturbed observations. *Mon. Wea. Rev. 130*, 1913–1924.

Whitaker, J. S., T. M. Hamill, X. Wei, Y. Song, and Z. Toth (2008). Ensemble data assimilation with the ncep global forecast system. *Mon. Wea. Rev. 136*, 463–482.

Zhang, F., C. Snyder, and J. Sun (2004). Impacts of initial estimate and observation availability on convective-scale data assimilation with an Ensemble Kalman Filter. *Mon. Wea. Rev. 132*, 1238–1253.